

DAMAGE DOSIMETER THIRD OCTAVE AND TIME HISTORY RMS VALUES

David Banaszak and Dansen Brown Air Force Research Laboratory (AFRL)

Dr. Angela Trego, P.E., The Boeing Company

KEYWORDS: Strain, Time History, Third Octave, Mean, Standard Deviation, Root Mean Square

ABSTRACT

The Air Force sponsored flight tests using damage dosimeters, fabricated by The Boeing Company, to measure temperature and structural dynamic strains on B-52, F-15 and C-130 aircraft. The dosimeter measurements help diagnose difficult-to-analyze structural conditions, such as acoustics and high cycle fatigue, and support the durability patch design process to repair secondary structure cracks. The dosimeter is a rugged, small, lightweight data acquisition unit that runs autonomously off of battery power. It measures 3 channels of strain at a rate up to 15 kilo-samples per second and 1 channel of temperature at a rate of 1.3 samples per second. The dosimeter acquires data above a programmer defined root mean square (rms) strain threshold. It is currently programmed to store 42 time history records (0.3 seconds each) and compute and store 29,544 third octave spectra (18 bands each) in its 4-megabyte memory. LabVIEW™ virtual instruments (VIs) provide a quick look at the time history and third octave data and stores mean, rms and standard deviation values into a spreadsheet. This paper compares rms values computed from third octave data with rms values from time history data.

1. Background and Theory

Aircraft damage resulting from a high cycle fatigue (HCF) environment of greater than 10^6 cycles is often referred to as nuisance cracks. Typical cracking of secondary aircraft structure is shown in figure 1. This damage results in costly inspection and repair. Design of a durability repair patch requires information characterizing temperature, resonant response frequency and strain levels. The durability patch and damage dosimeter program is an Air Force effort to resolve these problems by measuring the operating environment with a compact, stand-alone, electronics called a damage dosimeter and then applying a specifically-designed damped bonded repair patch. A composite bonded patch used by Roach (1998) is shown in figure 2.

Hardware and software details for the damage dosimeter can be found in Ikegami, Rogers, Haugse and Trego (2001) and Haugse, Johnson, Smith, Rogers and Ryan (1999). A dosimeter photo and

block diagram is shown in figures 3 and 4 respectfully. The dosimeter implements the Anderson Current Loop (ACL) signal conditioning technique described by Anderson (1995). Two types of data records are stored in the non-volatile memory of a dosimeter. A Strain Time History (TH) record consists of 2048 points of strain data sampled at 7600 samples per second for each of 3 channels. If the root mean square (rms) value of the data is above a predefined threshold, the dosimeter computes a Fast Fourier Transform (FFT) of each of the three strain time histories to generate a Power Spectral Density (PSD). The PSD is then integrated over 18 discrete third octave frequency bands to compress the strain data into contiguous third octave bands as described by Banaszak, Brown and Trego (2002). The 2048 points for the first 42 TH records above threshold are stored in the dosimeter's non-volatile flash memory. The third octave data are stored until memory is filled in Standard Data Records (SDRs). Table I from Ikegami, Rogers, Haugse and Trego (2001) shows the format of SDR and TH records in the 4-megabyte (MB) flash memory for the current dosimeter configuration.

As noted by Bain and Englebert (1992), basic statistical property for any probability distribution of a random variable X (strain) is that

$$E(X^2) = \text{rms}^2 = \mu^2 + \sigma^2 \quad (1)$$

where, $E(X^2) = \text{rms}^2 = \text{Expectation}(X^2)$, μ^2 is the mean square of X and σ^2 is the variance of X or σ is the standard deviation of X. For the dosimeter, let X = one of the 2048 sample points of a stored TH record, then $E(X^2) = \text{rms}^2$, μ^2 and σ^2 are easy to compute. For a time history, μ^2 is the steady (DC) portion of the time history and σ^2 is alternating (AC) portion of the time history and $E(X^2) = \text{rms}^2$ is the total of the DC plus the AC portion of the time history. For the dosimeter, equation (1) is easily verified by using a spreadsheet for any dosimeter TH record by computing $E(X^2)$, μ^2 and σ^2 . By design, the dosimeter's DC static component of the strain is $\mu^2 = 0$ so that $E(X^2) = \text{RMS}^2 = 0 + \sigma^2 = \sigma^2$.

One-third octave bands are stored in up to 29,455 SDR records. The starting point of the third octave band distribution is programmable. Practical limits on the starting point are between 15 Hz and 75 Hz. Below 15 Hz, the width of the third octave band is less than the frequency increment of 3.71 Hz ($= 7600\text{Hz} / 2048$). Above 75 Hz, the final third octave band lies above the Nyquist frequency of 3800 Hz ($=$

7600Hz / 2). The dosimeter records third octave band rms values for each strain gage.

The three steps to compute the third octave overall rms are (1) square each band rms to get the mean square, (2) sum all resultant band rms²s and (3) take the square root of that result to get to the overall rms. That is

$$\text{overall } rms^2 = \sum_{i=1}^{18} rms(i)^2 \quad (2)$$

where i is the band number. Equation (2) shows that bin center frequency knowledge is not required to compute the overall rms. But, remember that any energy outside the 1/3 octave bins (like the DC offset and frequencies greater than the maximum frequency band) are not included in the resulting third octave overall rms. Since the dosimeter is designed to have $\mu^2 = 0$, ideally the third octave overall rms value should equal the time history overall rms value. This paper will compare the rms levels of the 42 TH records with the first 42 SDR records by looking at the correlation and slope between the third octave standard deviation (σ_{SDR}) and the time history standard deviation (σ_{TH}). The dosimeter is designed to have $rms^2 = \sigma^2$ or $rms = \sigma$.

2. Dosimeter Data Acquisition Overview

The dosimeter data acquisition sequence described by Banaszak, Brown and Trego (2002) is shown in figure 5. The sequence includes first time threshold calculation, data collection, data processing, threshold comparison, and data recording. Acquired data are stored in memory as shown in table I. Table I shows that the current dosimeter stores the peak strain value in SDR records for each 2048 time history sample. Another important statistic to consider for future dosimeter storage is the crest factor = peak/rms.

Banaszak, Brown and Trego (2002) developed a LabVIEW™ virtual instrument (VI) that views the third octave and 42 TH records. This VI created the plots for each of the nine experimental test cases described later. In addition to displaying the dosimeter TH and SDR records, the VI computes and displays the overall rms (σ_{SDR}) for each strain gage from the third octave records and μ , rms and σ_{TH} for the 2048 samples of the TH records as seen in the close up view of C-130 data in figure 6. The VI also has an option to save the computed and recorded values for the TH and SDR records to a spreadsheet compatible file.

Table I. Content and Size of SDR and TH Records in Dosimeter Flash Memory

Standard Data Record		Strain Time-History Record	
Element	Size	Element	Size
Time	6 bytes	Time	10 bytes
Temperature	2 bytes	Unused	2 bytes
Strain Peaks	6 bytes	Temperature	2 bytes
1/3-Octave Bands Ch1	36 bytes	Strain Time-Hist Ch1	4096 bytes
1/3-Octave Bands Ch2	36 bytes	Strain Time-Hist Ch2	4096 bytes
1/3-Octave Bands Ch3	36 bytes	Strain Time-Hist Ch3	4096 bytes
Total Record Size	122 bytes	Total Record Size	12302 bytes
Memory First Address (hex)	10000	Memory First Address (hex)	380001
Memory Last Address (hex)	380000	Memory Last Address (hex)	400000
Total Memory	3604480 bytes	Total Memory	524287 bytes
Maximum Number of Records	29544	Maximum Number of Records	42
Records per Second	1.3	Records per Second	1.3
Maximum Recording Time	10.67 hours	Maximum Recording Time	54.60 seconds

3. Processing Time History and Third Octave Records 1-42 for Nine Experimental Cases

3.1 Three Aircraft Experimental Cases

The Boeing Company, in conjunction with AFRL, used the dosimeter to collect dynamics strain data on three aircraft. Time history and third octave data for the first 42 time history were compared for some of aircraft data collected from the C-130, B-52 and F-15. Preliminary third octave and time history plots for the aircraft experiments are shown in figure 7. Record number 1 for the three aircraft cases are in the top row of figure 7. For case (1) F-15 data, there is zero level third octave data for all bands and very low-level time history data. For case (2) B-52 data, there is some cyclic rms value in third octave band 8 and some cyclic content in the time history data. The strain overall rms level is still low. For case (3) C-130 data, there is cyclic rms value in third octave band 9 and all three strain gage time histories have an overall rms value greater than 15µε.

3.2 Six Laboratory Experimental Cases

Between November 2001 and January 2002, AFRL conducted six laboratory experiments to better understand the dosimeter operation. For three laboratory experiments, three strain gages mounted on an aluminum plate were excited on an electrodynamic shaker by sine or random inputs. In one experiment, the three strain gages were excited using a remote control structural exciter (RCSE) described by Banaszak (2001). On two experiments, shunt calibration resistors simulated 1000 micro strain (µε). The bottom two rows of figure 7 show typical laboratory dosimeter third octave and time history records. For case (4), a sinusoidal excitation of the shaker, there is a strong sinusoidal first bending mode of the plate in third octave band 9 for all three strain gages. The time histories have an overall rms value of 177 to 184 µε. For case (5), laboratory shaker noise when a taper recorder is turned on, there appears to be pickup of test equipment noise. Here we see the strong sinusoidal in third octave band 9 for all three strain gages. The time histories do not look random and have an overall rms value of 33 to 34 µε. For case (6), a RCSE excites the three strain gages on the

Case	Excitation	Signal Type	SG#	Correlation	Slope
1	F-15	Random	1	0	0
2	B-52	Sine+Random	1	0.9913	1.0085
3	C-130	Sine+Random	1	0.9785	0.985
4	LabShaker	Sine	1	0.9601	0.9826
5	LabShaker	Noise	1	0.9987	1.0531
6	LabRCSE	Sine	1	0.9805	0.2806
7	Shaker+SG1Shunt	Sine+Switch	1	0.9955	0.3747
8	Only4SGShunt	Switch	1	0.9435	0.3055
9	LabShaker	Random	1	0.9936	0.9885
1	F-15	Random	2	0	0
2	B-52	Sine+Random	2	0.9014	0.7562
3	C-130	Sine+Random	2	0.4408	0.2341
4	LabShaker	Sine	2	0.9489	0.9557
5	LabShaker	Noise	2	0.9986	1.0527
6	LabRCSE	Sine	2	0.9868	0.28
7	Shaker+SG1Shunt	Sine	2	0.8807	0.9964
8	Only4SGShunt	Switch	2	0.9447	0.3216
9	LabShaker	Random	2	0.9969	1.0798
1	F-15	Random	3	0	0
2	B-52	Sine+Random	3	0.9505	0.9725
3	C-130	Sine+Random	3	0.383	0.076
4	LabShaker	Sine	3	0.9596	0.9613
5	LabShaker	Noise	3	0.9982	1.0478
6	LabRCSE	Sine	3	0.9813	0.2781
7	Shaker+SG1Shunt	Sine	3	0.7381	0.9016
8	Only4SGShunt	Switch	3	0.9873	0.3079
9	LabShaker	Random	3	0.997	1.1788

Table II. Correlation and Slope Between σ_{SDR} and σ_{TH}

plate using vibrating pagers to generate a series of 1.3 second sinusoidal bursts at a frequency of about 145 hertz. Here we see the strong sinusoidal vibration induced in the plate in third octave band 9 for all three strain gages. The time histories have an overall rms value of 103 to 191 $\mu\epsilon$ rms. The time history shows that the dosimeter does not respond to DC since the 450 $\mu\epsilon$ peak in the time history is due to the transient when the RCSE is turned on. For case (7), a sinusoidal excitation of the shaker overlaying a shunt resistor static calibration of 1000 $\mu\epsilon$ on SG 1, we see the strong sinusoidal first bending mode of the plate in third octave band 9 for all three strain gages. The time history has an rms value of 123 to 131 $\mu\epsilon$. Again, since the dosimeter does not respond to DC, we do not see the 1000 $\mu\epsilon$ on SG 1, but just see the AC component. Case (8) features a switched 1000 $\mu\epsilon$ shunt calibration for Vref, SG1, SG2 and SG2 in sequence. Since the dosimeter only responds to DC, we see a decaying transient in the time history. The third octave plot indicates that the frequency content is mostly in the lower frequency band for all three strain gages. The time histories have an overall rms value of 365 to 368 $\mu\epsilon$. Lastly for case (9), a random excitation using white noise of DC-5kHz, we see the strong sinusoidal first bending mode of the plate is seen in third octave band 9 for all three strain gages. The time histories have an overall rms value of 30 to 32 $\mu\epsilon$. The plots show record 1, but data for all 42 time history and respective third octave records were used in the following analysis.

3.3 Converting Data from Dosimeter Memory to SAS[®] JMP[®]

This paper assumes that all nine experimental cases have the same strain calibration and the same sampling rate (7600 samples/sec). The process used to convert dosimeter memory data to SAS[®] JMP[®] (2000) file formats follows: (1) Download data from dosimeter memory to a computer file. (2) Use LabVIEW[™] VI to view records and to save as a spreadsheet file (extension .ssh). (3) Rename file extension to .txt. (4) Remove header line in Microsoft[®] Excel and save with .xls file extension. (5) Import .xls file to SAS[®] JMP[®] 4.0. (6) Delete records greater than 42 and save with .jmp file extension.

4 Statistical Analysis

4.1 Compute Correlations and Slopes for σ_{TH} and σ_{SDR} for Strain Gages 1-3

The σ_{SDR} and σ_{TH} of 42 records were computed using the LabVIEW[®] VI. They were stored in a SAS[®] JMP[®] (.jmp) file for each of the 9 cases. The following procedure was used to compute correlations and slopes for each of the nine cases. First open the file using SAS[®] JMP[®]. Then use the Analyse Multivariate, Correlation menus to get correlations between σ_{SDR} and σ_{TH} . Next use the fit Y by X to get slopes between third octave values and time history values. If all time history data is included in the third octave data, the slope between these should be 1.

4.2 Create a Table for Statistical Analysis

Next AFRL engineers entered correlations and slopes into a new table for each of the nine cases. Table II shows the correlations and slopes between the σ_{SDR} and σ_{TH} values. The case number, excitation and signal type are potential control factors. Case number is just a number of the 9 experimental cases. Classification of the vibration excitation includes aircraft (F-15, C-52 or C-130), laboratory shaker, remote control structural exciter or shunt resistor calibrator. Signal type is determined by using engineering judgment, based on the plots in figure 7, as to type of signal recorded. Potential blocking and nuisance factors need to be identified. These may include the dosimeter serial number or strain gage number. The response variables are the correlations and slopes between σ_{SDR} and σ_{TH} .

4.3 Analyses Y by X to Show Differences.

Using SAS[®] JMP[®] menus to analyse Y by X, the plots produced by oneway analysis of correlation and slope by case and by excitation are shown in figures 8 and 9. Figures 8 and 9 include mean

diamonds, which show the 95 % confidence interval for the means. An oneway analysis by strain gage number did not indicate any significant differences in the correlations and slopes. As seen in the figures, the correlation by excitation is close to one except for case (1), F-15 data, and case (3), C-130 data. The Tukey-Kremer 0.05 significant level multiple comparison circles confirm the significant differences in the F-15 correlation between third octave rms values and time history rms values. This verifies that for the first 42 records of F-15 data, that there was no rms energy in any of the third octave bands for the respective F-15 time history and hence zero correlation. Later F-15 records had non-zero rms values for the third octave bands but no time history information to compare.

When looking at the response variable slope versus case or excitation, there is a lot more scatter in the oneway analysis of slope plots. Ideally, the slope should be close to 1 for all cases. For case 2, 4, 5 and 9 this is true. However for cases 1,3,5,7 and 8, all the slopes appear to be less than one. This implies that some of the energy content in the time history signal is not being included in the third octave. Case (1), the F-15 is pretty obvious since there are no rms values in any of the third octave bands. Case 3 and 5 have pretty low-level rms values. Thus maybe most of the time history includes noise frequency data higher than the maximum third octave band. Case 7 and 8 included high-level static change in strain values. Since the dosimeter does not respond to static changes, a lot of lower frequency energy may not be included in the third octave data.

As shown by the nine experimental cases, the rms value of the third octave data and time history data are not necessarily equal. Some possible explanations include: (1) Not all time history frequencies are included in the third octave data. That is, the start and stop frequencies do not cover the dosimeter range of 0-5000 hertz. (2) Data may be sampled at less than the Nyquist frequency. (3) There were only 42 time histories per case. With increasing memory sizes, more time history records can be recorded. (4) The low rms levels in F-15 data implied 0 values in third octave bands. (5) Excitation type and amplitude level may have a significant impact. (6) The removal of DC in acquisition of TH data can add unwanted energy in the low frequency bands.

5. Summary and Conclusions

The damage dosimeter is a useful tool to get quick response definition of thermal and dynamic strain frequencies on military and commercial aircraft. The dosimeter needs update to measure static and dynamic measurements simultaneously. Flight usage

on a B-52, F-15, and C-130 shows that the dosimeter allows an engineer to easily instrument an in-service aircraft to obtain the structural characteristics necessary to properly select damping materials and design an arresting repair.

In addition to adding more memory, the dosimeter should store the mean, standard deviation and rms value for each time history record, in addition to the peak strain for each TH record, to help to quickly ascertain data quality.

Acknowledgments

David Smith and Karl Anderson helped to understand the dosimeter operation, Capt. Michael Myers an AFRL guided the dosimeter delivery to completion on contract F33615-95-D-3203 and Pat Huguenard set up laboratory evaluation equipment.

References

1. Anderson, K. F., (1995) "Practical Applications of Current Loop Signal Conditioning", Technical Memorandum: NASA-TM-4636, January, NASA Dryden Flight Research Facility, Edwards CA.
2. Bain & Englebert (1991) Introduction to Probability and Mathematical Statistics Second Edition, page 74, PWS-KENT, Boston, MA.
3. Banaszak, David (2001), "End-to-end Mechanical Calibration of Strain Channels in Dynamic Health Monitoring Systems", Institute of Environmental Sciences and Technology (IEST) 2001 Proceedings, 47TH ATM, Phoenix AZ, Mount Prospect, IL.
4. Banaszak, D., Brown, D. and Trego, A. (2001) "A Quick Look at Flight Data from a Digital Damage Dosimeter", Institute of Environmental Sciences and Technology ESTECH 2002 Proceedings, 48ATM, Mount Prospect, IL.
5. Haugse, E., Johnson, P.S., Smith, D. L., Rogers, L., Ryan, J., (1999) "Durability Patch & Damage Dosimeter: A Portable Battery Powered Data Acquisition Computer and Durability Patch Design Process", Third Joint FAA/DoD/NASA Conference on Aging Aircraft, Sep 20-23, Albuquerque, NM.
6. Ikegami, R., Rogers, L., Haugse, Trego, A., (2001), "Structural Technology and Analysis Program (STAP) Delivery Order Number: 004 Durability Patch", AFRL-VA-WP-TR-2001-3037 to be published.
7. Roach, Dennis P., (1998)



Figure 3. Dosimeter and Battery Pack

“Bonded Composite Doublers for Commercial Aviation Use”, *Aerospace Engineering*, pages 37-39, April.

8. SAS® Institute Inc. (2000) *JMP® Introductory Guide Version 4*, Gary, NC.



Figure 1. Cracks on Secondary Aircraft Structure

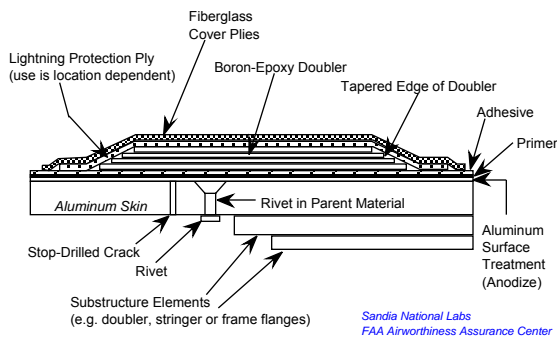


Figure 2. Bonded Composite Repair

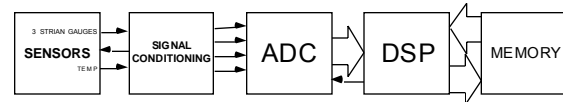


Figure 4. Dosimeter Block Diagram

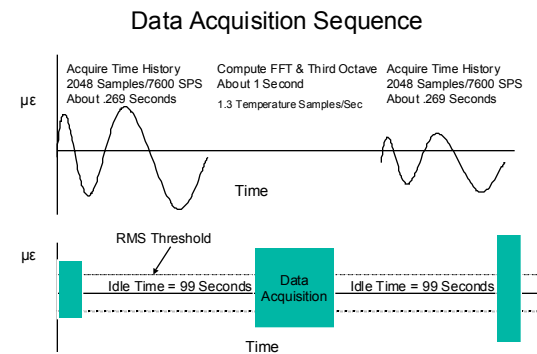


Figure 5. Dosimeter Data Acquisition Sequence

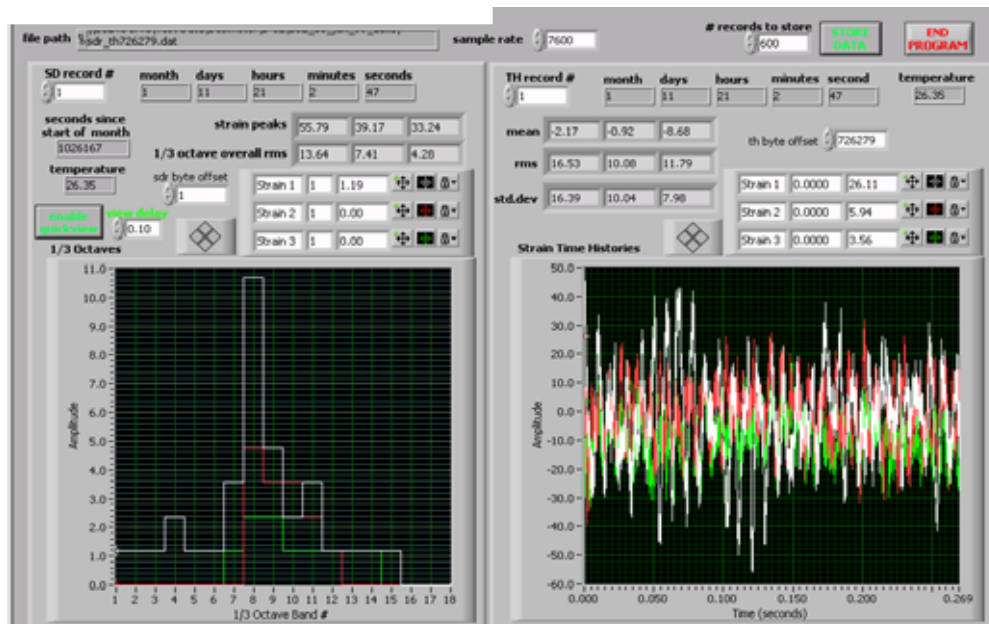


Figure 6. View of B-52 Sample Data Showing VI Computations

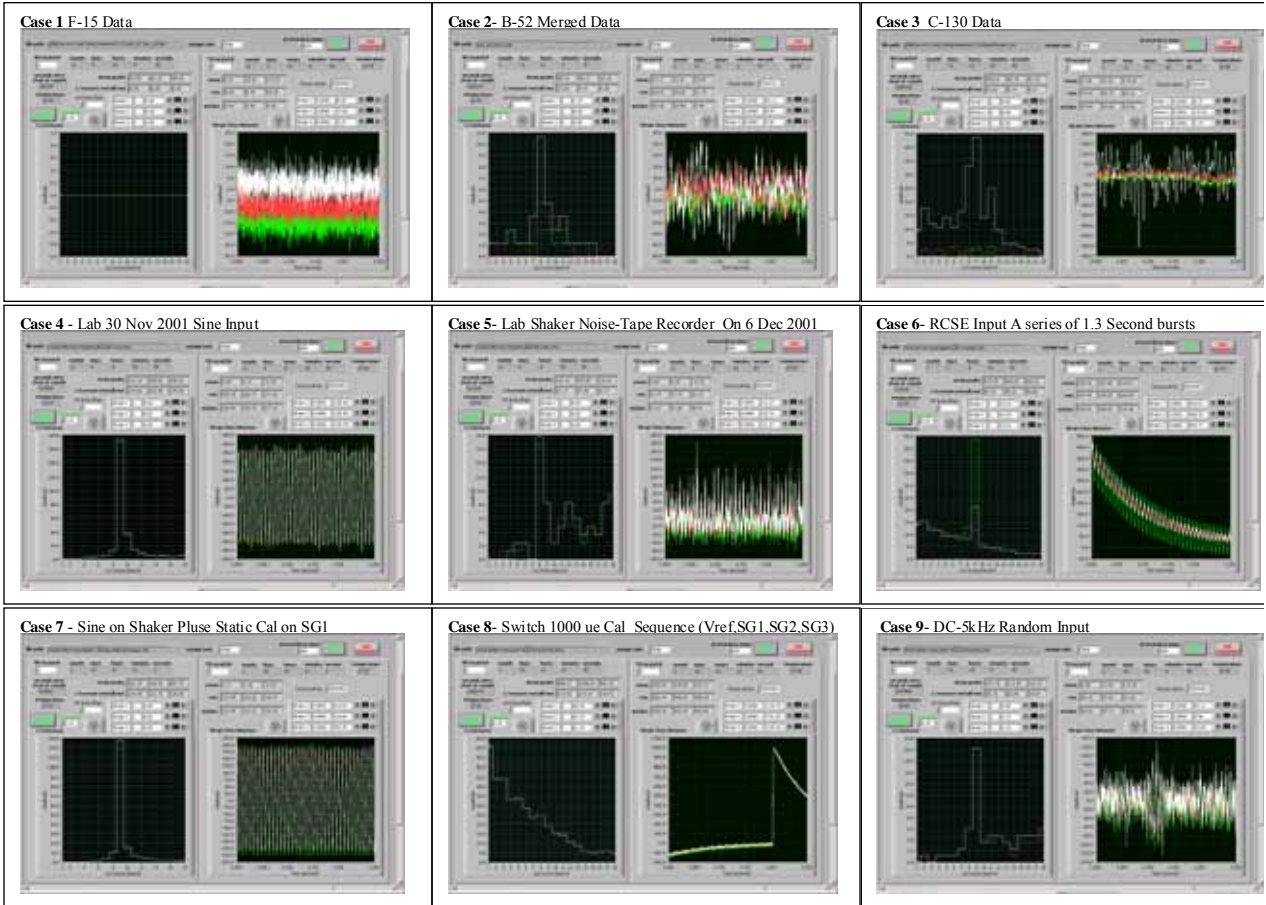


Figure 7. Nine Cases of Aircraft and Laboratory Dosimeter Data Acquisition

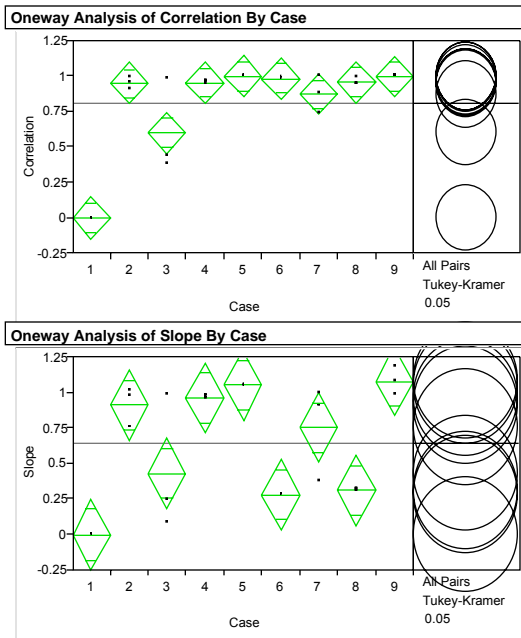


Figure 8. Correlation and Slope by Case

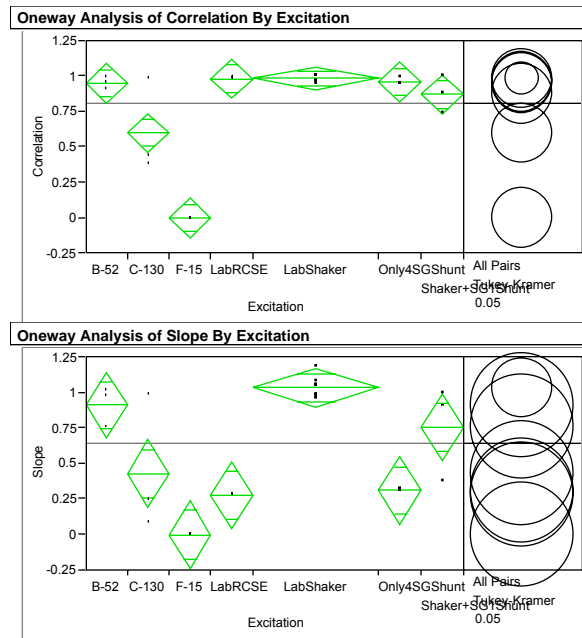


Figure 9. Correlation and Slope by Excitation